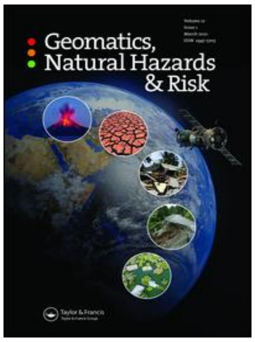

Taylor & Francis
Taylor & Francis Group

Geomatics, Natural Hazards and Risk

ISSN: (Print) (Online) Journal homepage: https://www.tandfonline.com/loi/tgnh20

Cyclone vulnerability assessment of the western coast of Bangladesh

Muhammad Al-Amin Hoque , Biswajeet Pradhan , Naser Ahmed , Bayes Ahmed & Abdullah M. Alamri

To cite this article: Muhammad Al-Amin Hoque , Biswajeet Pradhan , Naser Ahmed , Bayes Ahmed & Abdullah M. Alamri (2021) Cyclone vulnerability assessment of the western coast of Bangladesh, Geomatics, Natural Hazards and Risk, 12:1, 198-221, DOI: 10.1080/19475705.2020.1867652

To link to this article: https://doi.org/10.1080/19475705.2020.1867652

Published online: 06 Jan 2021.

GEOMATICS, NATURAL HAZARDS AND RISK
2021, VOL. 12, NO. 1, 198–221
https://doi.org/10.1080/19475705.2020.1867652

Cyclone vulnerability assessment of the western coast of Bangladesh

Muhammad Al-Amin Hoque[a,b], Biswajeet Pradhan[a,c,d], Naser Ahmed[b], Bayes Ahmed[e] and Abdullah M. Alamri[f]

[a]Centre for Advanced Modelling and Geospatial Information Systems (CAMGIS), School of Information, Systems and Modelling, University of Technology Sydney, Ultimo, NSW, Australia; [b]Department of Geography and Environment, Jagannath University, Dhaka, Bangladesh; [c]Department of Energy and Mineral Resources Engineering, Sejong University, Seoul, Republic of Korea; [d]Earth Observation Center, Institute of Climate Change, Universiti Kebangsaan Malaysia, Bangi, Selangor, Malaysia; [e]Institute for Risk and Disaster Reduction (IRDR), University College London (UCL), London, UK; [f]Department of Geology & Geophysics, College of Science, King Saud University, Riyadh, Saudi Arabia

ABSTRACT

Coastal Bangladesh is one of the hotspots of tropical cyclone's landfall in South Asia. A spatial vulnerability assessment is required to formulate disaster risk reduction strategies. This study develops a comprehensive tropical cyclone vulnerability mapping approach by applying Fuzzy Analytical Hierarchy Process (FAHP) and geospatial techniques and examines the spatial distribution of tropical cyclone vulnerability in the western coastal region of Bangladesh. We have selected 18 spatial criteria under the physical, social, and mitigation capacity categories as the components of vulnerability. Results indicate that the southern and south-eastern peripheral areas exhibit higher vulnerability to tropical cyclones since these areas comprise low elevation, gentle slope, closeness to the sea, a high number of historical cyclone tracks, vulnerable land cover classes (settlements and crops land), and poor socio-economic structures. These areas cover most of the Barguna, Khulna, Bagerhat, Jhalokati, and southern parts of Satkhira, and Pirojpur districts. The existing mitigation capacity measures, for example, the construction of cyclone shelters, embankments, road networks, and effective warning systems in these areas are not adequate levels. The findings would be useful for policymakers and local authorities in formulating appropriate cyclone risk mitigation plans in coastal Bangladesh.

ARTICLE HISTORY
Received 10 July 2020
Accepted 17 December 2020

KEYWORDS
Cyclone; vulnerability; fuzzy logic; AHP; GIS; remote sensing; Bangladesh

1. Introduction

Globally, tropical cyclones are considered as the most deadly meteorological hazards (Li and Li 2013; Needham et al. 2015). Strong winds, heavy precipitations, and storm

CONTACT Biswajeet Pradhan Biswajeet.Pradhan@uts.edu.au, biswajeet24@gmail.com

surges are notable destructive characteristics of tropical cyclones (Chen and Liu 2016; Sahoo and Bhaskaran 2018). These natural events often cause significant casualties, widespread damages to agriculture and properties, and disruptions to communication networks (Hoque et al. 2018; Mazumdar and Paul 2018; Saxena et al. 2013). On average, 90 tropical cyclones originate each year across the several cyclone basins worldwide (Bakkensen and Mendelsohn 2019; Mansour 2019). Tropical cyclone impacts are frequently observed in many coastal regions of the world. These cyclones caused about 1965 billion US dollars' worth of global damages between 1970 and 2019 (WMO 2020). Currently, the vulnerability of coastal people and their resources to tropical cyclone impacts are a big concern since the exposure is increasing rapidly (Alam and Dominey-Howes 2015; Sahoo and Bhaskaran 2018). Future climate change scenarios, particularly sea-level rise, may accelerate this vulnerability to a greater extent (Appelquist and Balstrøm 2015; Bakkensen and Mendelsohn 2019; Moon et al. 2019; Xu et al. 2015).

Tropical cyclones are very common in Bangladesh (Islam et al. 2013; Sattar and Cheung 2019). Bangladesh is bounded on the south by the Bay of Bengal where tropical cyclones are formed frequently in the Bay of Bengal during early summer (April to June) and late rainy season (September to November) (Paul 2009; Uddin et al. 2019). On average, 12 to 13 tropical depressions form in this Bay each year, and among them, five acquire the intensity of tropical cyclones (Paul et al. 2010). Most of these tropical cyclones hit the coastal areas of Bangladesh (Hoque et al. 2019; Karim and Mimura 2008). Bangladesh has a very prolonged history of tropical cyclones (Alam et al. 2020). Many of these cyclones have caused the coastal areas with large area destruction, loss of human lives, and extensive property damages (Alam et al. 2020; Hossain 2015). About 500,000 and 140,000 people have lost their lives by two notable tropical cyclones that made landfall in the coastal areas of Bangladesh in 1970 and 1991, respectively (Alam and Dominey-Howes 2015; Sattar and Cheung 2019). Cyclone Sidr that hit in 2007, killed 3,500 people and incurred around $1.67 billion US dollars' worth of economic loss (Alam et al. 2020). Cyclone Aila that made landfall in 2009 caused 190 deaths; injured 7000 people; and destroyed more than 500,000 houses (Ahmed et al. 2016). Due to low-lying coastal regions, many people will be at risk under the scenario of storm surges with future sea-level rise (Mullick et al. 2019; Rana et al. 2010).

Undertaking appropriate mitigation measures can reduce the loss and impacts of devastating tropical cyclones (Ahmed et al. 2016; Sattar and Cheung 2019). A comprehensive tropical cyclone vulnerability assessment can produce sufficient information to support effective mitigation measures (Hoque et al. 2017; Khan 2008; Saxena et al. 2013). Theoretically, vulnerability is defined as the extent of the susceptibility of the people, resources, and environments to the impacts of particular hazards which is determined by physical, social, economic, and environmental criteria (UNDRR 2009). Remote sensing data coupled with spatial analysis provides an efficient approach to assess the spatial tropical cyclone vulnerability (Hoque et al. 2017; Rao et al. 2013; Yin et al., 2013). Several criteria, directly and indirectly, influence the tropical cyclone vulnerability for any area (Mansour 2019). A vast amount of data in the form of spatial and non-spatial are required to evaluate the influence of criteria in the tropical cyclone vulnerability assessment (Mansour 2019). Several mapping approaches have been used for assessing spatial tropical cyclone vulnerability using geospatial techniques (Ali et al. 2020; Hoque et al. 2019; Mazumdar and Paul 2018; Rao et al. 2013). Multi-criteria integrating mapping techniques are considered best as these provide detailed spatial vulnerability information of tropical cyclone impacts (Alam et al. 2020; Ali et al. 2020). Among the spatial multi-criteria evaluation approaches, the Fuzzy Analytical Hierarchy Process (FAHP) is the most appropriate approach popularly used in the literature (Hategekimana et al. 2018; Tahri et al. 2017).

Although Bangladesh is considered a highly tropical cyclone-prone country, the studies related to tropical cyclone vulnerability assessment are very limited. Some studies are found focusing on the assessment of tropical cyclone risk (Alam et al. 2020; Hoque et al. 2018, 2019; Quader et al. 2017; Sattar and Cheung 2019), vulnerability (Alam and Collins 2010; Hossain 2015), impacts and adaptation (Karim and Mimura 2008; Mallick et al. 2017) in coastal Bangladesh. Quader et al. (2017) mapped the risk to human lives and livelihoods for the coastal areas of Bangladesh using limited criteria, largely focusing on social aspects. Hoque et al. (2018) developed a tropical cyclone model using multi-criteria approach at a local-scale. Recently, Hoque et al. (2019) and Alam et al. (2020) performed risk assessment of tropical cyclones on the eastern coast of Bangladesh using geospatial techniques. In contrast, Hossain (2015) analysed the vulnerability to tropical cyclone impacts at the household level using the qualitative data collected through the questionnaire survey from two villages of western coastal regions of Bangladesh. Future scenarios were modelled by Karim and Mimura (2008) for evaluating future climate change impacts on storm surges on the western coast of Bangladesh. Mallick et al. (2017) conducted a study to evaluate the coastal communities' adaptation, recovery, and preparedness to tropical cyclone impacts in some coastal villages of the south-western coast of Bangladesh. A comprehensive assessment of vulnerability by integrating adequate criteria of vulnerability elements, such as physical, social, and mitigation capacities, is essential to generate detailed and accurate vulnerability information (Cutter et al. 2003; Rashid 2013). To date, no study has been found on mapping spatial tropical cyclone vulnerability using multi-criteria evaluation incorporating the essential components of vulnerability covering the entire western coast of Bangladesh.

The aim of the present study is to develop a comprehensive tropical cyclone vulnerability mapping approach that incorporates physical and social vulnerability, and mitigation capacity. The proposed method examines the spatial distribution of tropical cyclone vulnerability in the western coastal zone of Bangladesh. This analysis is conducted focussing on three specific objectives: (1) to develop a physical vulnerability, social vulnerability, and mitigation capacity index of tropical cyclones using FAHP and geospatial approaches; (2) to prepare a vulnerability map integrating indices of physical and social vulnerabilities and mitigation capacity to examine the spatial distribution of tropical cyclone vulnerability, and (3) to validate the produced spatial vulnerability results.

2. Materials and methods

2.1. Method overview

In this study, we applied a FAHP based multi-criteria assessment approach to incorporate physical, social, anthropogenic, and mitigation capacity criteria for tropical

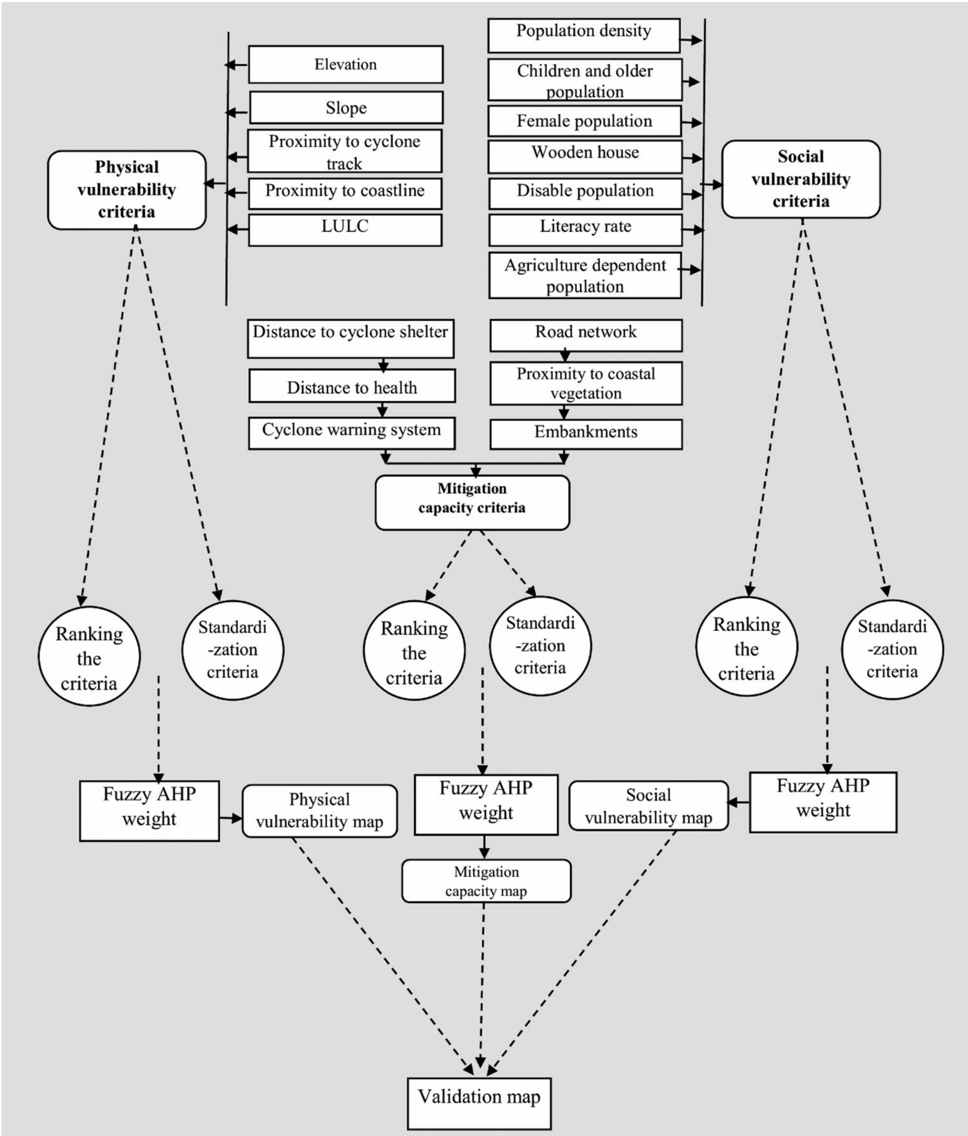

Figure 1. Systematic representations of the vulnerability assessment approach applied in the current study.

cyclone vulnerability assessment. Several vulnerability equations are reported in the scientific works for vulnerability assessment of natural hazards (Hoque et al. 2017). In this study, Eq. (1) was used based on the literature review for assessing tropical cyclone vulnerability (Dewan 2013; Rashid 2013).

$$\text{Vulnerability} = (\text{Physical vulnerability} \times \text{Social vulnerability})/\text{Mitigation capacity} \quad (1)$$

Figure 1 summarizes the methodological flowchart employed in the present study.

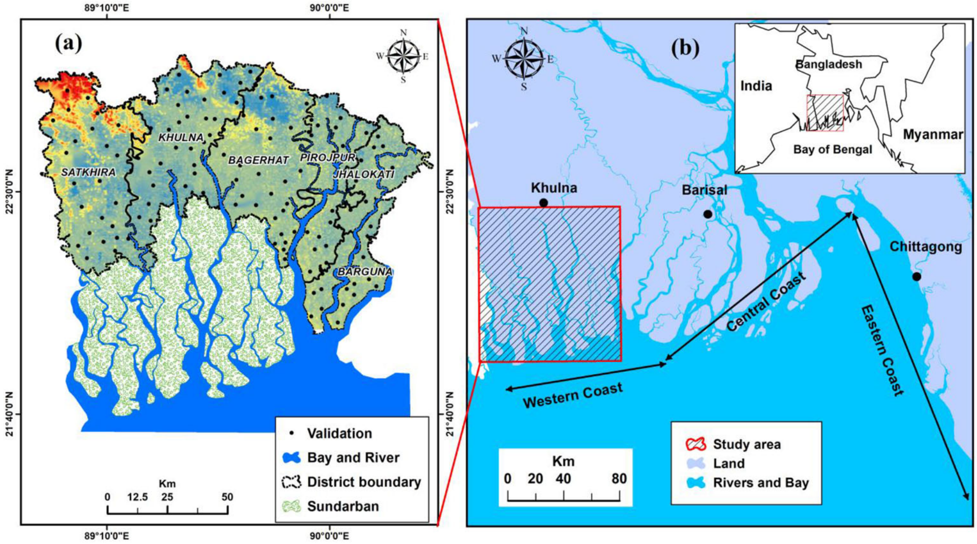

Figure 2. (a) Districts (administrative unit) boundary of the western coastal region, and (b) the study area in the context of the coastal zones of Bangladesh.

2.2. Study area

Following the physiographic units of Bangladesh, the coastal area is classified into western, central, and eastern coastal zones. In this study, we only considered the Ganges tidal deltaic plain, which is known as western coastal zone. However, to maintain consistency, we only selected six cyclone-prone districts and their 46 Upazilas of the western coastal zone with a total area of 9041.52 sq. km. The western coastal region of Bangladesh is geographically located between 22°00′–23°00′ N latitude and 89°00′–90°00′ E longitude (Figure 2). The total population of the region is 8,641,473, where 633 people live per square km (BBS 2012). The inhabitants of the western coast are highly vulnerable to natural disasters due to their socio-economic conditions and higher rates of poverty (Akter et al. 2019). A humid climate prevails in the area with an annual rainfall of 1940 mm. The study area is frequently affected by devastating tropical cyclones. The characteristics of topography and geographical location accelerate the strengths and higher occurrences of tropical cyclones (Hoque et al. 2018; Sattar and Cheung 2019). The western coastal zone is formed with a low-lying deltaic plain, wide rivers, and estuaries (Karim and Mimura 2008). Recently, the coast was severely affected by super Cyclone Sidr (2007) and Aila (2009), causing 3500 deaths and 191 injuries to the people with substantial damages to the properties and environment (Sattar and Cheung 2019). Although we included six coastal districts in this study, highly affected by previous tropical cyclones, the effects of cyclones could be extended beyond the study site along the north-south direction.

2.3. Dataset and sources

Several types of criteria were required to consider for assessing tropical cyclone vulnerability. The spatial data used to evaluate the criteria were generated from various

Table 1. Dataset with their characteristics used in the present analysis.

Data type	Source	Period	Purpose of uses
Sentinel 2 (10 m resolution)	United States Geological Survey (USGS) Earth explorer	Five Sentinel 2 images (November, 2018)	Land cover
RapidEye (5 m resolution)	DigitalGlobe foundation	Twelve Rapid Eye images (December, 2015 to January, 2016)	Coastal vegetation
Digital Elevation Model (DEM) at 20 m spatial resolution	Survey of Bangladesh (SOB)	2014	Elevation, slope
Population	Bangladesh Bureau of Statistics (BBS)	Population census 2011	Population density, dependent population, female population, wooden house, disable population, literacy rate, agriculture dependent population
Cyclone track	International Best Track Archive for Climate Stewardship (IBTrACS)	1960–2018	Proximity to cyclone track, cyclone frequency
Road, Embankment	LGED	2018	Road network, Embankments,
Cyclone shelter, health infrastructure, cyclone warning system	LGED and Fieldwork		Distance to cyclone shelter and health infrastructure, cyclone warning system

sources using geospatial techniques. The data sources included national, international, government, and private institutions as well as fieldwork. Mitigation capacity and validation data were collected using several field investigations between 2015 and 2020. Table 1 details the datasets with their types, sources, period, and specific uses.

2.4. Criteria for vulnerability assessment

The criteria and sub-factors were chosen in this study using a literature review and their relevance and influence on tropical cyclone vulnerability. We developed 18 spatial criteria layers in the geospatial environment under three components, including physical, social, and mitigation capacity for cyclone vulnerability assessment. Each raster layer has a $30\,\text{m} \times 30\,\text{m}$ spatial resolution. ArcGIS and ENVI software were used in preparing and processing criteria layers. The produced maps were classified using the natural break classification approach that was found more suitable to visualize the spatial pattern of vulnerability in this study (Baeza et al. 2016; Tehrany et al. 2014). The following paragraphs detail the mapping procedures and significance of the chosen criteria.

2.4.1. Criteria for physical vulnerability

Some physical phenomena/factors that influence tropical cyclone vulnerability were chosen for this study. The selected factors/criteria included elevation, slope, proximity to cyclone track and coastline, and land cover (Dewan 2013; Gallina et al. 2016; Rimba et al. 2017 S V et al., 2018).

Elevation and slope are vital factors for tropical cyclone vulnerability assessment (Ali et al. 2020). The vulnerability is considered less for the areas characterized by

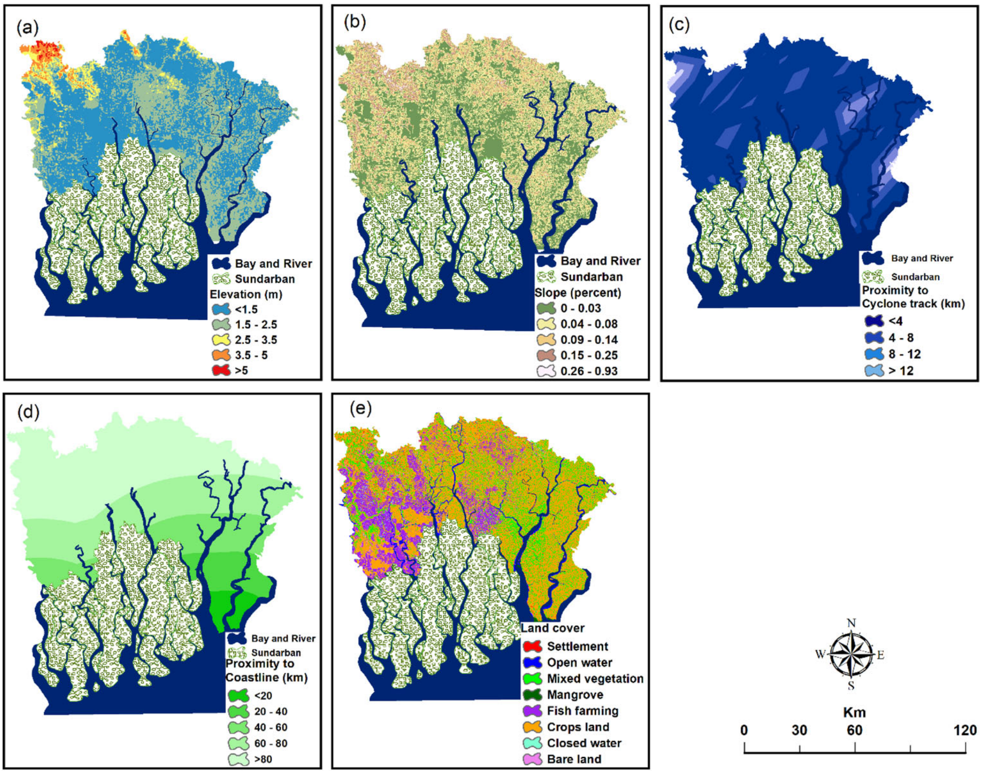

Figure 3. Physical vulnerability criteria: (a) elevation, (b) slope, (c) proximity to cyclone track, (d) proximity to coastline, and (e) land cover.

high elevation and steep slope (Li and Li 2013). In contrast, the areas with a low elevation and gentle slope are designated for the higher vulnerability (Yin et al. 2010 ; Yin et al., 2013). The elevation and slope maps were generated using a 20-m spatial resolution digital elevation model (DEM) (Figure 3a and 3b). The DEM was prepared using the topographic sheet (scale 1: 25,000) collected from the Survey of Bangladesh. The Z accuracy of the DEM was +/− 50 cm.

The vulnerability to tropical cyclones is high for lives and properties located close to past cyclone tracks and the coastline (Alam et al. 2020). Therefore, proximity to cyclone tracks and coastline criteria were considered for assessing the physical vulnerability to tropical cyclones. The data of International Best Track Archive for Climate Stewardship (IBTrACS) were used to develop the buffers and map the distance from cyclone tracks (Figure 3c) (Knapp et al. 2010). A total of 30 spatial cyclone tracks ranging from category 1–5 cyclones were found over the study area between 1968 and 2019 from the cyclone track datasets and used in the buffer analysis. In contrast, distances from the coastline of the study area were calculated using the ruler tool of Google Earth Pro. Next, the proximity to coastline spatial layer was produced (Figure 3d).

Some types of land covers are highly susceptible to tropical cyclones. We used five Sentinel-2 images to prepare land cover spatial layers (Figure 3e). Firstly, the required pre-processing corrections such as geometric, radiometric, and atmospheric

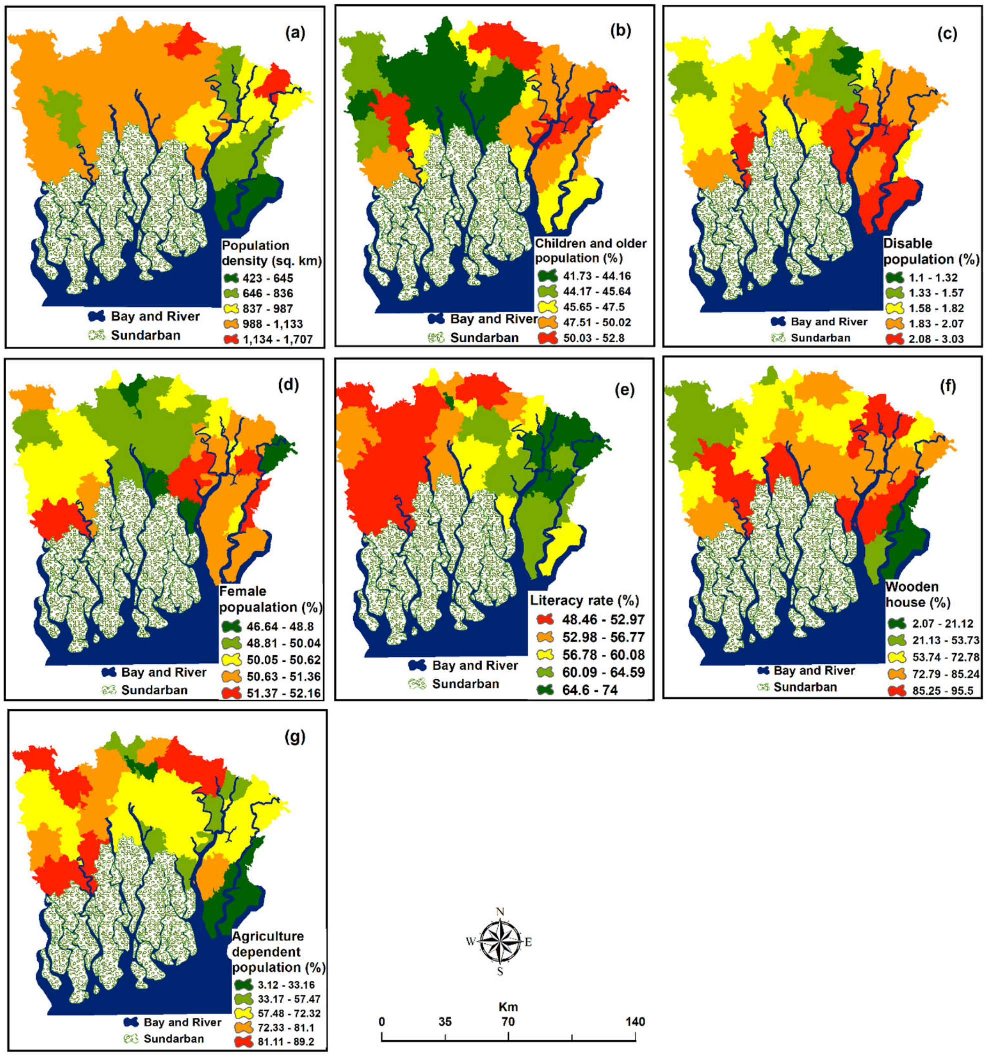

Figure 4. Social vulnerability assessment criteria: (a) population density, (b) dependent population, (c) disable population, (d) female population, (e) literacy rate, (f) wooden house, and (g) agriculture dependent population.

corrections were applied to the satellite images, and then a hybrid classification approach was used to identify land cover categories, e.g. mixed vegetation, settlement, fish farming, open water bodies, mangrove vegetation, crops land, closed water bodies and bare land. Initially, unsupervised classification was applied to identify the probable classes, and then a maximum likelihood algorithm was used under the supervised classification technique (Kumar et al. 2013). Very-high resolution Google Earth Imagery (2019) was used to generate 513 random points to assess the accuracy of the land cover map. Next, accuracy assessment technique was performed based on the literature (Hoque et al. 2016; Jensen 2005). Subsequently, 91.03% and 89.74% were found as overall accuracy and Kappa coefficient, respectively.

2.4.2. Criteria for social vulnerability

Some social factors that influence tropical cyclone vulnerability were chosen in this study. The selected factors/criteria included population density, unemployed population, disabled population, female population, literacy rate, wooden house, and agricultural dependent population. We used the latest available population and housing census data (2011) to prepare all the social factors related spatial layers. The population and housing census is conducted in Bangladesh within 10 years' interval, and the next round of census will be conducted in 2021.

The population in coastal areas is increasing faster across the world (Neumann et al. 2015). Devastating coastal hazards like tropical cyclones are becoming a big concern for the coastal people. The social vulnerability to tropical cyclones is largely controlled by spatial variation of population density in a given area. The densely populated areas have a high-vulnerability to tropical cyclones compared to the less populated area (Ali et al. 2020). On the other hand, children and older population categories are highly impacted by tropical cyclones as they have limited capability to follow and implement emergency measures effectively without any assistance during the evacuation . This study used the population and housing census data (2011) from the Bangladesh Bureau of Statistics (BBS) to prepare the population density as well as children and older population spatial layers (Figure 4a and 4b).

Disabled people are considered highly vulnerable to tropical cyclones. Many disabled people cannot promptly follow evacuation procedures without the help of others. Many times, they are unable to get an early warning system and any kind of support during the disaster emergency period. In addition, the impacts of tropical cyclone disasters are comparatively higher in the Bangladeshi female population compared to their male counterparts. This is because they face difficulties and challenges for their limited mobility, knowledge, access to resources, and other issues, including security prior to disaster emergency (Alam and Rahman 2014; Neumayer and Plümper 2007). In this study, we prepared the disabled and female population spatial layers using the latest census data (Figure 4c and 4d).

Literacy rate plays a vital role in determining social vulnerability to cyclone disasters. The literate people are more aware of the impacts of cyclones and are more likely to follow the evacuation procedures and other preparedness activities to minimize the probable impacts (Muttarak and Lutz 2014). In this study, we used the population and housing census data of 2011 to prepare the literacy rate spatial layer (Figure 4e).

House structure and their inhabitants are impacted by tropical cyclones. The houses in the study area is dominated by wooden houses, which are more vulnerable to damage from tropical cyclones induced wind speed, intense rainfall, and storm surges. Therefore, wooden house was taken as a criterion. We prepared the wooden house spatial layers categorizing into five groups (Figure 4f). In contrast, storm surges, strong winds, and heavy precipitation cause damage to agricultural crops (Hoque et al. 2016). Consequently, agricultural dependent people face a massive loss of income by the tropical cyclone impacts. We prepared the agricultural dependent spatial layer by classifying the percentages of dependency into five categories (Figure 4g). We extracted the data for analysing both of these criteria from the population and housing census of 2011.

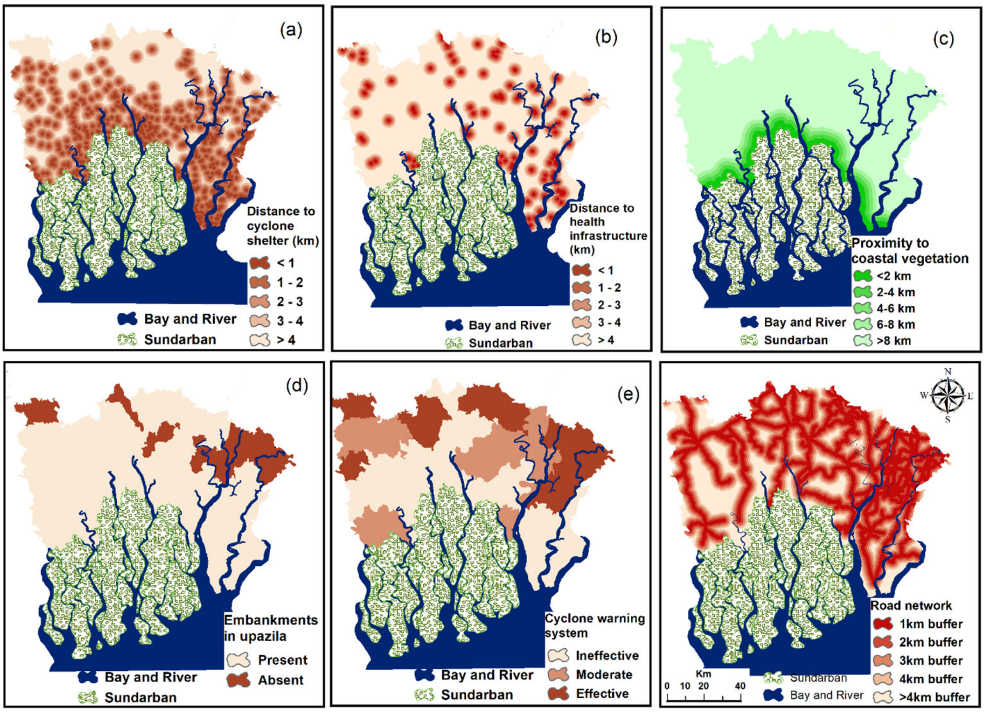

Figure 5. Mitigation capacity criteria: (a) distance to cyclone shelter, (b) distance to health infrastructure, (c) proximity to coastal vegetation, (d) embankments, and (e) cyclone warning system and road network.

2.4.3. Criteria for mitigation capacity

Mitigation capacity of tropical cyclones hazards reflects the key plan, including structural and non-structural measures, to lessen the probable impacts of tropical cyclones (Mansour 2019). In this study, we selected the distance to cyclone shelter, health infrastructure, proximity to coastal vegetation, embankments, and road network criteria under the structural mitigation measures. On the other hand, the cyclone warning system criterion was chosen under non-structural mitigation measures.

Cyclone shelter works as a best structural mitigation measure that provides temporary shelter to affected communities prior to the cyclone disasters (Hoque et al. 2019). Similarly, health infrastructures support essential emergency health care to affected individuals during cyclone events (Ali et al. 2020). For this study, we collected the cyclone shelter data from the local government engineering department (LGED) and verified during multiple field visits from 2015–2020. Afterward, we applied the Euclidian distance techniques to measure the distances and generate distance to cyclone shelter and health infrastructure spatial layers (Figure 5a and 5b).

Coastal vegetation provides protection to people, properties, and environments by decreasing the impacts of strong winds and storm surges (Ali et al. 2020; Das and Vincent 2009). The spatial vegetation data acquired from the Bangladesh forest department were used to identify the areas under coastal vegetation in the study site. To generate the proximity to coastal vegetation, we used Euclidean distance tools in ArcGIS based on the identified coastal vegetation of the study area (Figure 5c). The

Table 2. Sub-criteria ranking scheme based on the relative importance of tropical cyclone vulnerability.

		Ranking (based on vulnerability)				
Component	Criteria	Very low (1)	Low (2)	Moderate (3)	High (4)	Very high (5)
Physical vulnerability	Elevation (m)	>5	3.5–5	2.5–3.5	1.5–2.5	<1.5
	Slope (%)	0.26–0.93	0.14–0.25	0.09–0.14	0.04–0.08	0–0.03
	Proximity to cyclone track (km)	>8	6–8	4–6	2–4	<2
	Proximity to coastline (km)	>80	60–80	40–60	20–40	<20
	Land cover	Open water bodies, bare land	Closed water bodies	Mixed vegetation, Mangrove	Crops land, Fish farming	Settlements.
Social vulnerability	Population density (sq km.)	423–646	646–836	837–987	988–1133	1134–1707
	Dependent population (%)	41.73–44.16	44.17–45.64	45.65–47.5	47.65–50.02	50.03–52.8
	Disabled population (%)	1.1–1.32	1.33–1.57	1.58–1.82	1.83–2.07	2.08–3.03
	Female population (%)	46.64–48.8	48.81–50.4	50.5–50.62	50.63–51.36	51.37–51.16
	Literacy rate (%)	64.6–74	60.09–64.59	56.78–60.08	52.98–56.77	48.46–52.97
	Wooden house (%)	2.07–21.12	21.13–53.73	53.74–72.78	72.79–85.24	85.25–95.5
	Agriculture dependent population (%)	<33.16	33.17–57.47	57.48–72.32	72.33–81.1	81.11–89.2
Mitigation capacity	Distance to cyclone shelter (km)	<1	1–2	2–3	3–4	>4
	Distance to health infrastructure (km)	<1	1–2	2–3	3–4	>4
	Proximity to coastal vegetation	<2	2–4	4–6	6–8	>8
	Embankments		Present		Absent	
	Cyclone warning system		Effective warning system	Moderate warning system	Ineffective warning system	
	Road network (km)	<1	1–2	2–3	3–4	>4

regions close to coastal vegetation are likely to be less susceptible to cyclones as they work as natural shields. In addition, embankments play a vital role in protecting agricultural crops and houses from the inundation of tropical cyclone-induced storm surges (Mullick et al. 2019). The present study used the presence or absence of embankments from LGED data to create the spatial layer of embankment (Figure 5d).

An appropriate warning system is vital to deliver up-to-date approaching cyclone disaster information and to prepare individual people to evacuate from the vulnerable places to tropical cyclones (Akhand 2003). We collected the warning system data that include the warning system structure, equipment, and personnel involved from the local administrative offices and analysed them to identify the pattern and classify following the various variables of the local warning system. We verified the analysed data in the field and processed it into three categories under the effective, moderate, and ineffective warning system following local administrative units in creating spatial layer (Figure 5e).

Road network helps to provide relief, rescue work, and other management activities before, during, and after the tropical cyclone events (Amin et al. 2019). The data of the major roads were acquired from the LGED, and the spatial layer of road network was prepared using the Euclidean distance tool (Figure 5f).

2.5. Ranking of sub-factors

To rank the sub-factors, we classified each criterion following two classification techniques, such as natural break (for elevation, slope, etc.) and manual classification (proximity to cyclone track, road network, etc.). Afterward, the sub-factors under each criterion were ranked into five vulnerability levels (1–5), indicating very-low vulnerability (rank 1) and very-high vulnerability (rank 5) following the assumption that higher the vulnerability—higher the ranking value (Table 2). For ranking sub-factors, we used block units for social criteria. However, the social criteria were later converted to raster format with a similar cell value in order to maintain consistency between physical and social criteria. All the ranked spatial criteria layers were transformed into 30 m resolution spatial individual raster layers. Raster criteria layers were then standardized to bring the rank values of spatial criteria layers on the same scale (0 to 1). The standardization procedure was performed using Eq. (2).

$$p = \frac{x - \min}{-\min} \qquad (2)$$

where p refers to the standardized score, min and max represent the minimum and maximum values associated with each dataset, and x indicates the cell value in each spatial raster layer.

2.6. FAHP and criteria weighting

This study adopted the FAHP to weight the criteria since FAHP assists the decision-makers in overcoming uncertainty in providing the preferences of alternatives in the decision-making process (Kannan et al. 2013; Ku et al. 2010). Previous studies

Table 3. Membership function of linguistic scale.

Linguistic variable	Crisp number	Triangular fuzzy numbers	Reciprocal triangular fuzzy numbers
Equally strong	1	(1,1,1)	(1,1,1)
Moderately strong	3	(2,3,4)	(1/4,1/3,1/2)
Strong	5	(4,5,6)	(1/6,1/5,1/4)
Very strong	7	(6,7,8)	(1/8,1/7,1/6)
Extremely strong	9	(9,9,9)	(1/9, 1/9, 1/9)
Intermediate	2	(1,2,3)	(1/3,1/2,1)
	4	(3,4,5)	(1/5,1/4,1/3)
	6	(5,6,7)	(1/7,1/6,1/5)
	8	(7,8,9)	(1/9,1/8,1/7)

employed various FAHP approaches (Hadipour et al. 2020; Hategekimana et al. 2018; Tahri et al. 2017). However, an integrated FAHP procedure was followed in this study that was developed by Chang (1996). A triangular fuzzy number (TFN) is used to simplify the pair-wise comparison in this approach to avoid the complex comparing procedure. The five steps FAHP method (Chang 1996) adopted in the study to determine the criterion weight is explained below.

In the first step, the relevant criteria for mapping tropical cyclone vulnerability assessments were selected.

In step 2, pair-wise comparison matrices were constructed based on the relative importance of selected criteria adopting a geometric mean method to incorporate the six expert's opinions as following Eq. (3). Judgments of experts/decision-makers are the primary source to weigh the criteria based on their importance regarding the spatial problem. These judgments are represented qualitatively by some linguistic variables. In this stage, a fuzzy set is required to quantify the judgments by using the respective membership function. A triangular fuzzy set was used for converting the linguistic variables to the quantitative values in this study. The relationship between quantitative values and linguistic variables are shown in Table 3.

$$R = (a, b, c), K = 1, 2, ..., K (R\text{: triangular fuzzy member and } K\text{: no. of DMs}) \quad (3)$$

$$\text{where } a = (a_1 \times a_2 \times \cdots \times a_k)^{\frac{1}{k}},$$

$$b = (b_1 \times b_2 \times \cdots \times b_k)^{\frac{1}{k}}, \; c = (c_1 \times c_2 \times \cdots \times c_k)^{\frac{1}{k}}$$

Then in step three, pair-wise comparison matrices were aggregated and synthesized to develop a set of overall priorities for the hierarchy.

In step four, the consistency ratio (CR) was calculated to justify expert's ratings in the pair-wise matrices. The judgment is considered true if the consistency ratio is equal to or less than 0.1. To measure the CR, Eq. (4) was adopted:

$$\text{CR} = \text{Consistency Index}/\text{Random Index}, \quad (4)$$

where the random index (RI) is calculated based on the matrix order (n) provided by Saaty (1980). In addition, consistency index (CI) is calculated by Eq. (5):

Table 4. Criteria weights from pair-wise comparison matrices along with CR values.

Component	Criteria	Weight
Physical vulnerability	Elevation	0.217
	Slope	0.208
	Proximity to coastline	0.220
	Proximity to cyclone track	0.217
	Land use and land cover	0.140
Consistency ratio (CR): 0.03		
Social vulnerability	Population density	0.194
	Dependent population	0.1781
	Female population	0.1764
	Wooden house	0.1695
	Disable population	0.1197
	Literacy rate	0.0975
	Agriculture dependent population	0.0649
Consistency ratio (CR): 0.01		
Overall vulnerability	Physical vulnerability	0.667
	Social vulnerability	0.333
Mitigation capacity	Distance to cyclone shelter	0.267
	Distance to health infrastructure	0.051
	Proximity to coastal vegetation	0.187
	Cyclone warning system	0.183
	Embankment	0.068
	Road network	0.193

Consistency ratio (CR): 0.01

$$CI = (\lambda_{\max} - n)/(n - 1), \tag{5}$$

where $\lambda_{\max}$ and n indicate the largest eigenvalue and order of a matrix, accordingly (Mahapatra et al. 2015).

In step five, pair-wise matrix criteria weights were transformed into linguistic variables using Table 3. The priority weights were calculated following the Chang (1996) method (Table 4).

2.7. Vulnerability assessment

The overlay analysis was used separately with the relevant criteria spatial layers and their weights to prepare the physical, social, and mitigation capacity indices. We then categorized the indices into five levels from very-low to very-high to obtain the physical, social, and mitigation capacity maps. Later, we produced a vulnerability index without integrating mitigation capacity by multiplying the physical and social vulnerability indices. On the other hand, a vulnerability index integrating mitigation capacity was prepared using Eq. (1). Both indexes values were then standardized to transform into a common scale 0 to 1 and classified them into several vulnerability levels, i.e. very-low, low, moderate, high, and very-high.

2.8. Validation of cyclone vulnerability approach

In this study, we applied the receiver operating characteristics curve (ROC) and the area under the curve (AUC) to validate the cyclone vulnerability map without integrated mitigation capacity. ROC AUC is an appropriate technique for the assessment of the effectiveness of deterministic and probabilistic justification (Youssef et al.

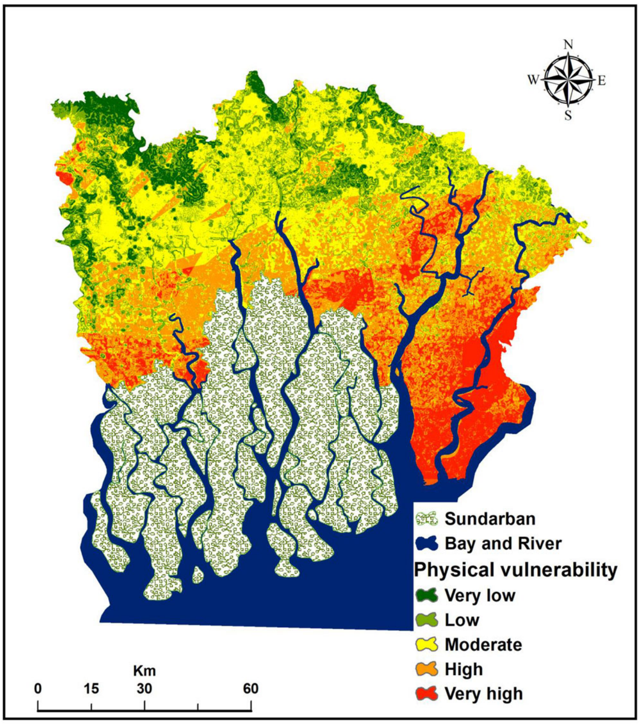

Figure 6. Spatial pattern and level of physical vulnerability to tropical cyclones.

Table 5. Area coverage of vulnerability and relevant components classes.

	Physical vulnerability		Social vulnerability		Mitigation capacity		Vulnerability without mitigation capacity		Vulnerability integrated mitigation capacity	
Class	Area (km^2)	%	Area (km^2)	%	Area (km^2)	%	Area (km^2)	%	Area (km^2)	%
Very-high	1332.3	14.7	2511.8	27.8	1368.2	15.1	1565.9	17.3	911.1	10.1
High	2502.3	27.7	1949.9	21.6	2359.7	26.1	2400.9	26.6	2067.5	22.9
Moderate	2874.0	31.8	1243.7	13.8	2517.7	27.8	2567.1	28.4	2689.7	29.7
Low	1716.8	19.0	2011.2	22.2	1955.7	21.6	1765.8	19.5	2281.0	25.2
Very-low	615.2	6.8	1325.0	14.7	839.3	9.3	740.7	8.2	1091.3	12.1

2016). This technique has been widely used for validating the vulnerability, susceptibility, and risk models of various natural hazards like floods, landslides, and droughts (Bui et al. 2019; Hoque et al. 2020; Khosravi et al. 2018; Nohani et al. 2019). Until now, there is no established approach to verify the map of tropical cyclone vulnerability. Consequently, we used the ROC AUC technique. Initially, we marked the areas that were affected by previous cyclones to create an inventory map (Figure 9) with 137 validation points based on existing studies' results (Hoque et al. 2016; Kumar Bhowmik and Cabral 2013), published reports ('Emergency Response and Action Plans Interim Report' prepared by Government of People's Republic of Bangladesh 2007 and 'Cyclone Sidr 2008 in Bangladesh' Prepared by the Government of Bangladesh) as well as fieldwork. The developed inventory map was used to

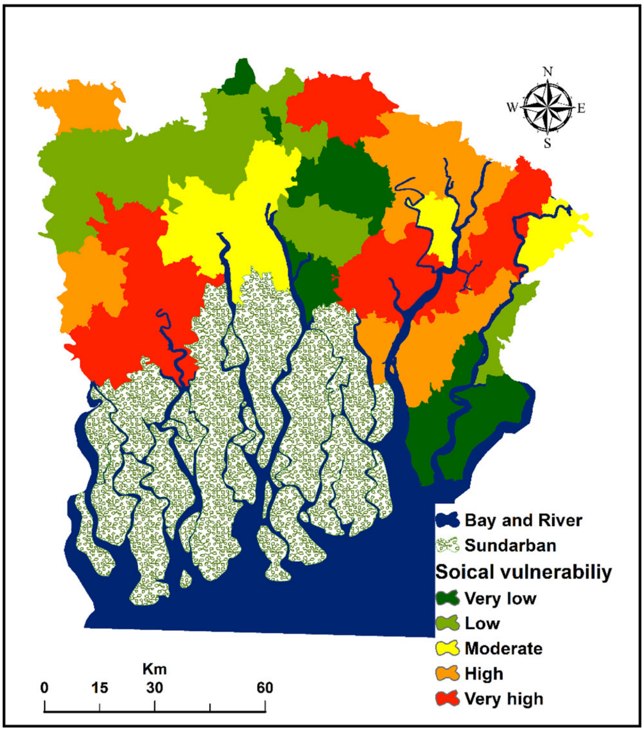

Figure 7. Spatial pattern and the level of social vulnerability to tropical cyclones.

generate prediction rate curve. 100% of cyclone-affected locations were used as a validation dataset to create a prediction rate curve.

3. Results and discussion

3.1. Spatial distribution of physical vulnerability criteria

Figure 6 illustrates the physical vulnerability to tropical cyclones classified into five classes. The prepared map exhibited that almost half (42.4%) of the study area has fallen into high to very-high physical vulnerability classes. In comparison, the very-high, and high vulnerability classes covered 14.7% and 27.7%, respectively (Table 5). The southern, south-western, and eastern parts, more specifically, the majority part of Satkhira, Khulna, Bagerhat, Jhalokati as well as Barguna district revealed high, and very-high vulnerability levels to cyclone impacts. Several important factors, such as low elevation, flat slope, very close to the coastline, an immense number of cyclone tracks and vulnerable land cover classes, are accountable for very-high physical vulnerability in those regions. On the contrary, only north-western and few segments from the central and eastern regions, particularly some parts of Satkhira, Bagerhat, and Pirojpur districts, depicted low to very-low vulnerability levels, which covered just 26% (2332 sq. km) of the study area combined (Table 5). Besides, more than 30% of the study area covered a moderately vulnerable class and found in the central and northern regions.

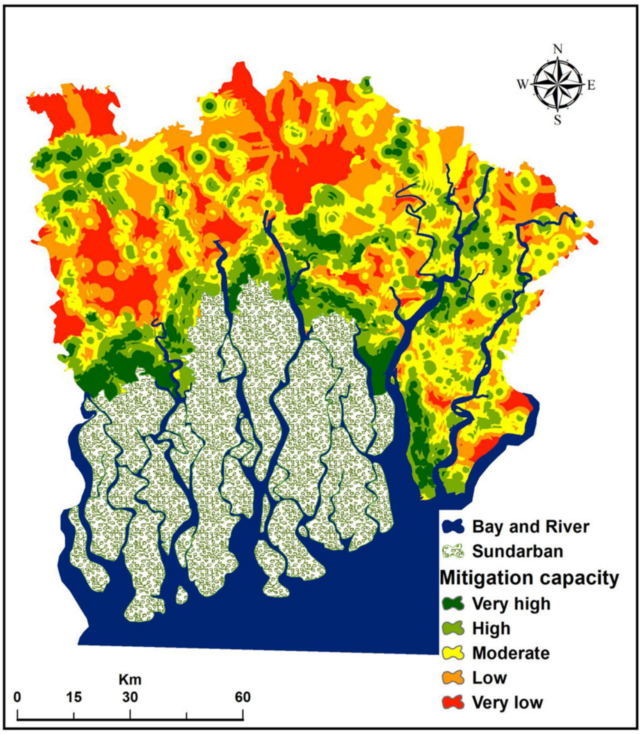

Figure 8. Spatial pattern of cyclone vulnerability mitigation capacity.

3.2. Spatial distribution of social vulnerability criteria

A very to high social vulnerability was observed in the areas of southern, south-western, and north-eastern parts (Figure 7). These areas are characterized with a high population density with many dependent, female, and illiterate people. However, the least covered class of social vulnerability mapping is the moderate vulnerable category, which covers about 1243.7 sq. km and consists of just 13.8% of the study area (Table 5). Moreover, over 36% of the area belongs to low to very-low vulnerable class and covered slightly over 2011.2 sq. km, and 1325 sq. km, accordingly and located in the south-eastern, north-western, and central parts (Table 5). These communities are found mostly on the southern and north-eastern portion and also have a better socio-economic condition compared to other regions.

3.3. Spatial distribution of mitigation capacity criteria

It is noticed from Figure 8 that around 69% of the study area (6245.6 sq. km) covers moderate to very-high mitigation capacity levels, whereas very-high mitigation capacity makes-up just 15.1% (1368.2 sq. km) of the study area (Table 5). Besides, about 28% and 26% of the study area exhibits moderate and high mitigation capacity, respectively. These areas include the southern, south-eastern, central, and western parts, particularly covering the district of Satkhira, Khulna, and some regions of Bagerhat and Barguna. However, low to very-low mitigation capacity categories occupy a considerable amount of portion

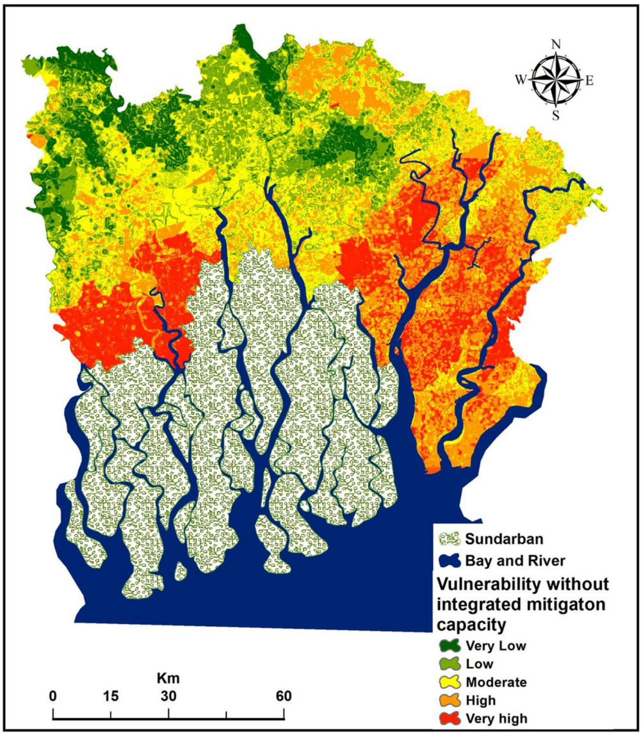

Figure 9. Spatial distribution and level of vulnerability derived from the incorporation of physical and social vulnerabilities to tropical cyclones.

(31% of the area) of the study site with the area over 1955.7 sq. km and 839 sq. km, respectively. These areas are found in the western part and in the southern region, more specifically, covering Khulna, Bagerhat, and few areas of Jhaokati districts (Table 5). Inadequate cyclone shelter, health facilities, embankments, and less effective warning systems are mainly responsible for this very poor mitigation capacity.

3.4. Vulnerability without integrated mitigation capacity

From Figure 9, it is observed that about 72% of the study area falls under moderate to very-high vulnerable classes, whereas around 17% (1566 sq. km) and 26% (2401 sq. km) areas are found in the category of very-high and high vulnerability, respectively (Table 5). These zones are identified in most parts of the Satkhira, Khulna, Bagerhat, Jhalokati, and some areas of Barguna and Pirojpur districts, and found in the study areas of southern and south-eastern segments. These regions consist of low elevation, gentle slope, closeness to the sea, high number of cyclone tracks, vulnerable land cover class, and poor socio-economic structures. Besides, low to very-low vulnerable areas are found in study areas northern and north-western parts and account for about 19% and 8% of the total areas, accordingly and located particularly in the north portion of Satkhira, Pirojpur and Barguna districts (Table 5). Due to high elevation, steeper slope, away from the coastline, fewer cyclone tracks, and well-developed socio-economic conditions resulted in these areas as less vulnerable zones.

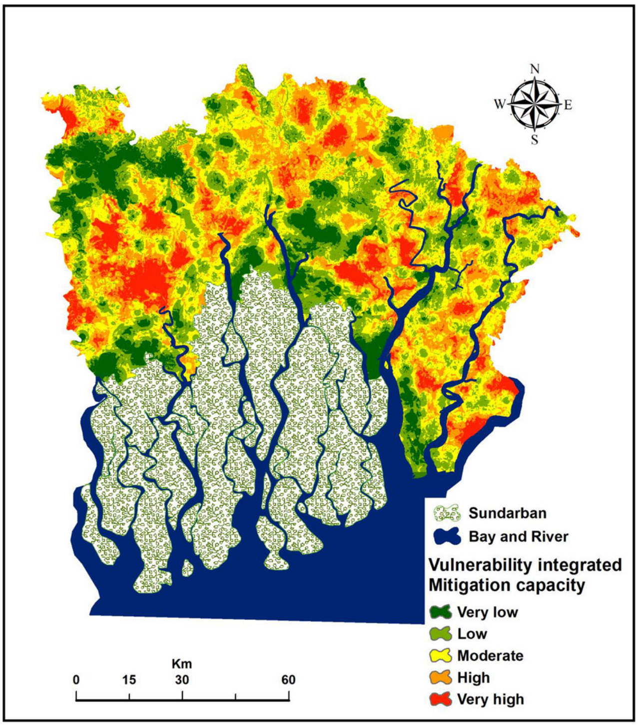

Figure 10. Spatial pattern and level of vulnerability derived from the incorporation of physical and social vulnerabilities and mitigation capacity to tropical cyclones.

3.5. Vulnerability integrated mitigation capacity

The developed cyclone vulnerability map with mitigation capacity shows a different pattern of findings from the vulnerability assessment without mitigation capacity and highlights locations where limited mitigation capacity alters the vulnerability assessment (Figure 10). In this map, the dispersed areas of the southern, south-eastern, and eastern parts are classified as moderate to very-low vulnerable category and cover around 67% (6062 sq. km) of the study area which are previously classified mostly as high to very-high vulnerable classes without mitigation capacity. Thus, incorporation of mitigation capacity is very crucial for deriving the actual vulnerable situation and provides information about where stronger mitigation measures are required. On the contrary, the largest portion of Khulna and Jhalokati districts and some portion of Satkhira, Bagerhat, and Barguna districts remained highly vulnerable because of inadequate mitigation capacity. Table 5 exhibits that the high vulnerable zone covers around 23% (2067 sq. km), whereas very-high vulnerable class covers about 10% (911 sq. km) of the study area.

3.6. Validation of cyclone vulnerability approach

The prediction rate curve is detailed in Figure 11 presenting model performance used in this study. AUC of the prediction rate for the FAHP model was 0.81 explaining 81.1% AUC prediction accuracy for the applied model. The values of AUC range between 0.5 to 0.1, further detailing values close to 1 shows higher accuracy (Youssef et al. 2016).

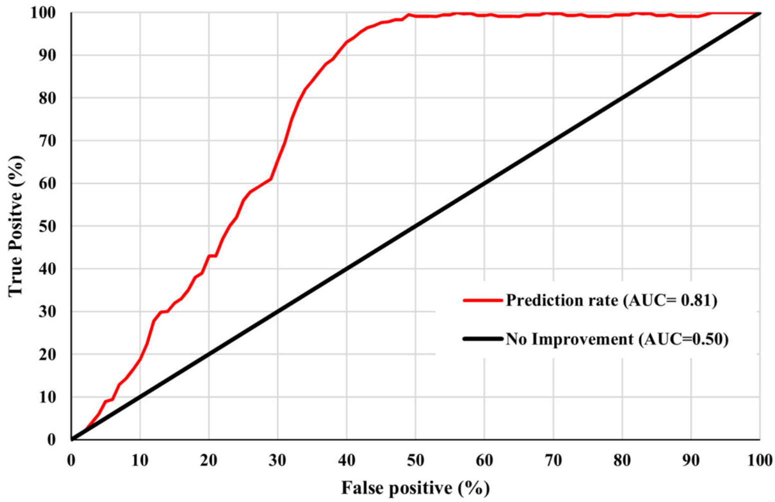

Figure 11. Area under the curve for prediction rate (81.1%).

Therefore, AUC value of prediction rate (81.1%) of this analysis presents the successful performance of our developed cyclone vulnerability assessment approach.

4. Conclusions

This research developed a comprehensive tropical cyclone vulnerability mapping approach and examined the spatial distribution of tropical cyclone vulnerability in the western coastal zone (9041.52 sq. km) of Bangladesh. Three components of vulnerability, namely, physical, social, and mitigation capacity, and their relevant criteria were integrated to examine the spatial vulnerability using geospatial and FAHP techniques, probably for the first time in this region. The ROC and AUC were successfully applied to validate the spatial vulnerability map. The cyclone vulnerability map without integrated mitigation capacity shows that most parts of Barguna, Khulna, Bagerhat, Jhalokati districts entirely covering the middle and southern parts of these areas; and some southern parts of Satkhira, and Pirojpur districts are highly vulnerable to tropical cyclone impacts. Our findings show that, with the incorporation of existing mitigation capacity, the area situated in the southern, south-eastern, western, and central portion (Khulna and Jhalokati districts and some portion of Satkhira, Bagerhat and Barguna district) remained highly vulnerable because of inadequate mitigation capacity. Consequently, the results of this study can be used to formulate and implement mitigation strategies where mitigation measures are not at the appropriate level to reduce future cyclone impacts.

Multi-criteria based analysis is a very effective technique for cyclone vulnerability mapping and was used in the present study. However, we faced challenges in collecting the most up-to-date and high-quality datasets. For example, we used social data from the latest population and housing census, which was conducted in 2011 for processing the criteria of social vulnerability. We had no choice but to use these old data since the next round of census will be conducted in 2021. Further, remote sensing data quality used for preparing elevation, slope (20 m resolution DEM), and LULC (Sentinel 10 m spatial resolution) were not at the satisfactory level due to low resolution. The cyclone shelter, embankment, and cyclone warning system datasets were acquired from LGED and local government offices. However, these data are not updated regularly. Thus, the possibility of missing some latest data may exist. However, we verified some of these data to include the latest information during the field visits. Further studies are required to address these limitations.

Despite having some drawbacks , this study is useful in real-world scenarios to formulate and implement cyclone risk mitigation strategies in the vulnerable areas of western coastal regions of Bangladesh. The probable cyclone mitigation measures could be increasing the cyclone shelter and health facilities, incorporating nature-based solutions, improving early warning system mechanisms, afforestation along the coast as well as the construction of seal wall or dykes. The applied and validated approach in this study could be used in other similar environment for tropical cyclone vulnerability assessment, adjusting a few factors and data types.

Acknowledgment

We are grateful to the Bangladesh Meteorological Department (BMD), Survey of Bangladesh (SoB), Local Government Engineering Department (LGED), Bangladesh Bureau of Statistics (BBS), International Best Track Archive for Climate Stewardship, and the United States Geological Survey (USGS), for providing the necessary datasets.

Disclosure statement

No potential conflict of interest was reported by the authors.

Funding

This research was supported by the Centre for Advanced Modelling and Geospatial Information Systems (CAMGIS), Faculty of Engineering and IT, the University of Technology Sydney (UTS), Australia. This research was also partially supported by the 'Researchers Supporting Project' (RSP-2020/14), King Saud University, Riyadh, Saudi Arabia.

ORCID

Biswajeet Pradhan http://orcid.org/0000-0001-9863-2054
Naser Ahmed http://orcid.org/0000-0003-2775-0592

References

Ahmed B, Kelman I, Fehr H, Saha M. 2016. Community resilience to cyclone disasters in coastal Bangladesh. Sustainability. 8(8):805.

Akhand MH. 2003. Disaster management and cyclone warning system in Bangladesh, Early warning systems for natural disaster reduction. Springer, Berlin, Heidelberg, p. 49–64.

Akter M, Jahan M, Kabir R, Karim DS, Haque A, Rahman M, Salehin M. 2019. Risk assessment based on fuzzy synthetic evaluation method. Sci Total Environ. 658:818–829.

Alam E, Collins AE. 2010. Cyclone disaster vulnerability and response experiences in coastal Bangladesh. Disasters. 34(4):931–954.

Alam E, Dominey-Howes D. 2015. A new catalogue of tropical cyclones of the northern Bay of Bengal and the distribution and effects of selected landfalling events in Bangladesh. Int J Climatol. 35(6):801–835.

Alam K, Rahman MH. 2014. Women in natural disasters: a case study from southern coastal region of Bangladesh. Int J Disaster Risk Reduct. 8:68–82.

Alam A, Sammonds P, Ahmed B. 2020. Cyclone risk assessment of the Cox's Bazar district and Rohingya refugee camps in southeast Bangladesh. Sci Total Environ. 704:135360.

Ali SA, Khatun R, Ahmad A, Ahmad SN. 2020. Assessment of cyclone vulnerability, hazard evaluation and mitigation capacity for analyzing cyclone risk using GIS technique: a study on Sundarban Biosphere Reserve. Earth Syst Environ. 4(1):71–92.

Amin S, Tamima U, Amador-Jiménez LE. 2019. Optimal pavement management: resilient roads in support of emergency response of cyclone affected coastal areas. Transp Res Part A Policy Pract. 119:45–61.

Appelquist LR, Balstrøm T. 2015. Application of a new methodology for coastal multi-hazard-assessment & management on the state of Karnataka, India. J Environ Manage. 152:1–10.

Baeza C, Lantada N, Amorim S. 2016. Statistical and spatial analysis of landslide susceptibility maps with different classification systems. Environ Earth Sci. 75(19):1318.

Bakkensen LA, Mendelsohn RO. 2019. Global tropical cyclone damages and fatalities under climate change: an updated assessment, hurricane risk. Springer, p. 179–197.

BBS. 2012. Housing and population census 2011, Bangladesh Bureau of Statistics (BBS), Ministry of Planning, Government of Bangladesh.

Bui DT, Tsangaratos P, Ngo P-TT, Pham TD, Pham BT. 2019. Flash flood susceptibility modeling using an optimized fuzzy rule based feature selection technique and tree based ensemble methods. Sci Total Environ. 668:1038–1054.

Chang D-Y. 1996. Applications of the extent analysis method on fuzzy AHP. Eur J Oper Res. 95(3):649–655.

Chen W-B, Liu W-C. 2016. Assessment of storm surge inundation and potential hazard maps for the southern coast of Taiwan. Nat Hazards. 82(1):591–616.

Cutter SL, Boruff BJ, Shirley WL. 2003. Social vulnerability to environmental hazards. Social Sci Q. 84(2):242–261.

Das S, Vincent JR. 2009. Mangroves protected villages and reduced death toll during Indian super cyclone. Proc Natl Acad Sci USA. 106(18):7357–7360.

Dewan AM. 2013. Vulnerability and risk assessment, floods in a megacity. Dordrecht: Springer, p. 139–177.

Gallina V, Torresan S, Critto A, Sperotto A, Glade T, Marcomini A. 2016. A review of multi-risk methodologies for natural hazards: consequences and challenges for a climate change impact assessment. J Environ Manage. 168:123–132.

Hadipour V, Vafaie F, Kerle N. 2020. An indicator-based approach to assess social vulnerability of coastal areas to sea-level rise and flooding: a case study of Bandar Abbas city, Iran. Ocean Coastal Manage. 188:105077.

Hategekimana Y, Yu L, Nie Y, Zhu J, Liu F, Guo F. 2018. Integration of multi-parametric fuzzy analytic hierarchy process and GIS along the UNESCO World Heritage: a flood hazard index, Mombasa County, Kenya. Nat Hazards. 92(2):1137–1153.

Hoque MA-A, Phinn S, Roelfsema C, Childs I. 2016. Assessing tropical cyclone impacts using object-based moderate spatial resolution image analysis: a case study in Bangladesh. Int J Remote Sens. 37(22):5320–5343.

Hoque MA-A, Phinn S, Roelfsema C, Childs I. 2017. Tropical cyclone disaster management using remote sensing and spatial analysis: a review. Int J Disaster Risk Reduct. 22:345–354.

Hoque MA-A, Phinn S, Roelfsema C, Childs I. 2018. Assessing tropical cyclone risks using geospatial techniques. Appl Geogr. 98:22–33.

Hoque MA-A, Pradhan B, Ahmed N, Roy S. 2019. Tropical cyclone risk assessment using geospatial techniques for the eastern coastal region of Bangladesh. Sci Total Environ. 692:10–22.

Hoque MA-A, Pradhan B, Ahmed N. 2020. Assessing drought vulnerability using geospatial techniques in northwestern part of Bangladesh. Sci Total Environ. 705:135957

Hossain MN. 2015. Analysis of human vulnerability to cyclones and storm surges based on influencing physical and socioeconomic factors: evidences from coastal Bangladesh. Int J Disaster Risk Reduct. 13:66–75.

Islam MN, Malak MA, Islam MN. 2013. Community-based disaster risk and vulnerability models of a coastal municipality in Bangladesh. Nat Hazards. 69(3):2083–2103.

Jensen JR. 2005. Introductory digital image processing: a remote sensing perspective. Upper Saddle River (NJ): Prentice-Hall Inc.

Kannan D, Khodaverdi R, Olfat L, Jafarian A, Diabat A. 2013. Integrated fuzzy multi criteria decision making method and multi-objective programming approach for supplier selection and order allocation in a green supply chain. J Cleaner Prod. 47:355–367.

Karim MF, Mimura N. 2008. Impacts of climate change and sea-level rise on cyclonic storm surge floods in Bangladesh. Global Environ Change. 18(3):490–500.

Khan MSA. 2008. Disaster preparedness for sustainable development in Bangladesh. Disaster Prev Manage. 17(5):662–671.

Khosravi K, Pham BT, Chapi K, Shirzadi A, Shahabi H, Revhaug I, Prakash I, Bui DT. 2018. A comparative assessment of decision trees algorithms for flash flood susceptibility modeling at Haraz watershed, northern Iran. Sci Total Environ. 627:744–755.

Knapp KR, Kruk MC, Levinson DH, Diamond HJ, Neumann CJ. 2010. The international best track archive for climate stewardship (IBTrACS) unifying tropical cyclone data. Bull Amer Meteor Soc. 91(3):363–376.

Ku C-Y, Chang C-T, Ho H-P. 2010. Global supplier selection using fuzzy analytic hierarchy process and fuzzy goal programming. Qual Quant. 44(4):623–640.

Kumar Bhowmik A, Cabral P. 2013. Cyclone Sidr impacts on the Sundarbans floristic diversity. ESR. 2(2):62–79.

Kumar P, Singh BK, Rani M. 2013. An efficient hybrid classification approach for land use/ land cover analysis in a semi-desert area using ${\rm ETM}{+} $and LISS-III sensor. IEEE Sens J. 13(6):2161–2165.

Li K, Li GS. 2013. Risk assessment on storm surges in the coastal area of Guangdong Province. Nat Hazards. 68(2):1129–1139.

Mahapatra M, Ramakrishnan R, Rajawat AS. 2015. Coastal vulnerability assessment using analytical hierarchical process for South Gujarat coast. Nat Hazards. 76(1):139–159.

Mallick B, Ahmed B, Vogt J. 2017. Living with the risks of cyclone disasters in the south-western coastal region of Bangladesh. Environments. 4(1):13.

Mansour S. 2019. Geospatial modelling of tropical cyclone risks to the southern Oman coasts. Int J Disaster Risk Reduct. 40:101151.

Mazumdar J, Paul SK. 2018. A spatially explicit method for identification of vulnerable hotspots of Odisha, India from potential cyclones. Int J Disaster Risk Reduct. 27:391–405.

Moon I-J, Kim S-H, Chan JC. 2019. Climate change and tropical cyclone trend. Nature. 570(7759):E3–E5.

Mullick MRA, Tanim A, Islam SS. 2019. Coastal vulnerability analysis of Bangladesh coast using fuzzy logic based geospatial techniques. Ocean Coastal Manage. 174:154–169.

Muttarak R, Lutz W. 2014. Is education a key to reducing vulnerability to natural disasters and hence unavoidable climate change? E&S. 19(1):42–50.

Needham HF, Keim BD, Sathiaraj D. 2015. A review of tropical cyclone-generated storm surges: global data sources, observations, and impacts. Rev Geophys. 53(2):545–591.

Neumann B, Vafeidis AT, Zimmermann J, Nicholls RJ. 2015. Future coastal population growth and exposure to sea-level rise and coastal flooding-a global assessment. PloS One. 10(3): e0118571.

Neumayer E, Plümper T. 2007. The gendered nature of natural disasters: the impact of catastrophic events on the gender gap in life expectancy, 1981–2002. Ann Assoc Am Geogr. 97(3):551–566.

Nohani E, Moharrami M, Sharafi S, Khosravi K, Pradhan B, Pham BT, Lee S, Melesse AM. 2019. Landslide susceptibility mapping using different GIS-based bivariate models. Water. 11(7):1402.

Paul B. 2009. Why relatively fewer people died? The case of Bangladesh's Cyclone Sidr. Nat Hazards. 50(2):289–304.
Paul BK, Rashid H, Islam MS, Hunt LM. 2010. Cyclone evacuation in Bangladesh: tropical cyclones Gorky (1991) vs. Sidr (2007). Environ Hazards. 9(1):89–101.
Quader MA, Khan AU, Kervyn M. 2017. Assessing risks from cyclones for human lives and livelihoods in the coastal region of Bangladesh. IJERPH. 14(8):831.
Rana M, Gunasekara K, Hazarika M, Samarakoon L, Siddiquee M. 2010. Application of remote sensing and GIS for cyclone disaster management in coastal area: a case study at Barguna district, Bangladesh. International archives of the photogrammetry. Remote Sens Spatial Inf Sci. XXXVIII(Part 8):122–126.
Rao VR, Subramanian BR, Mohan R, Kannan R, Mageswaran T, Arumugam T, Rajan B. 2013. Storm surge vulnerability along Chennai–Cuddalore coast due to a severe cyclone Thane. Nat Hazards. 68(2):453–465.
Rashid AKMM. 2013. Understanding vulnerability and risks. In: Shaw R, Mallick F, Islam A, editors. Disaster risk reduction approaches in Bangladesh. Disaster risk reduction. Japan: Springer, p. 23–43.
Rimba AB, Setiawati MD, Sambah AB, Miura F. 2017. Physical flood vulnerability mapping applying geospatial techniques in Okazaki City, Aichi Prefecture. Jpn Urban Sci. 1(1):7.
S V S S, Roy P S, V C, G S R. 2018. Flood risk assessment using multi-criteria analysis: a case study from Kopili River Basin, Assam, India. Geomatics Nat. Hazards Risk. 9(1):79–93. doi: 10.1080/19475705.2017.1408705.
Saaty T. 1980. The analytic hierarchy process. New York: McGraw-Hill International.
Sahoo B, Bhaskaran PK. 2018. Multi-hazard risk assessment of coastal vulnerability from tropical cyclones - A GIS based approach for the Odisha coast. J Environ Manage. 206:1166–1178.
Sattar MA, Cheung KK. 2019. Tropical cyclone risk perception and risk reduction analysis for coastal Bangladesh: household and expert perspectives. Int J Disaster Risk Reduct. 41:101283.
Saxena S, Purvaja R, Suganya GMD, Ramesh R. 2013. Coastal hazard mapping in the Cuddalore region, South India. Nat Hazards. 66(3):1519–1536.
Tahri M, Maanan M, Maanan M, Bouksim H, Hakdaoui M. 2017. Using Fuzzy Analytic Hierarchy Process multi-criteria and automatic computation to analyse coastal vulnerability. Prog Phys Geogr. 41(3):268–285.
Tehrany MS, Pradhan B, Jebur MN. 2014. Flood susceptibility mapping using a novel ensemble weights-of-evidence and support vector machine models in GIS. J Hydrol. 512:332–343.
Uddin M, Li Y, Cheung KK, Nasrin ZM, Wang H, Wang L, Gao Z. 2019. Rainfall contribution of tropical cyclones in the Bay of Bengal between 1998 and 2016 using. TRMM Satell Data Atmos. 10(11):699.
UNDRR. 2009. 2009 UNISDR terminology on disaster risk reduction, Geneva, Switzerland.
WMO. 2020. 2020 state of climate services, Switzerland.
Xu X, Sun D, Guo T. 2015. A systemic analysis of typhoon risk across China. Nat Hazards. 77(1):461–477.
Yin J, Yin Z, Xu S. 2013. Composite risk assessment of typhoon-induced disaster for China's coastal area. Nat Hazards. 69(3):1423–1434. doi:10.1007/s11069-013-0755-2.
Yin J, Xu S, Wang J, Zhong H, Hu Y, Yin Z, Wang K, Zhang X. 2010. Vulnerability assessment of combined impacts of sea level rise and coastal flooding for China's coastal region using remote sensing and GIS, Geoinformatics. 2010 18th International Conference on IEEE, p. 1–4.
Youssef AM, Pradhan B, Sefry SA. 2016. Flash flood susceptibility assessment in Jeddah city (Kingdom of Saudi Arabia) using bivariate and multivariate statistical models. Environ Earth Sci. 75(1):12.